Journal of Inorganic Biochemistry 168 (2017) 55–66

Contents lists available at ScienceDirect

Journal of Inorganic Biochemistry

journal homepage: www.elsevier.com/locate/jinorgbio

An unlikely DNA cleaving agent: A photo-active trinuclear Cu(II) complex based on hexaazatriphenylene

Dominique E. Williams [a], Christina M. Fischer [a], Miki Kassai [a], Lourdes Gude [b], María-José Fernández [b], Antonio Lorente [b,*], Kathryn B. Grant [a,*]

[a] Department of Chemistry, Georgia State University, P.O. Box 3965, Atlanta, GA 30302-3965, United States
[b] Departamento de Química Orgánica y Química Inorgánica, Universidad de Alcalá, 28871-Alcalá de Henares, Madrid, Spain

ARTICLE INFO

Article history:
Received 12 September 2016
Received in revised form 20 November 2016
Accepted 9 December 2016
Available online 15 December 2016

Keywords:
Copper(II)
DNA
Hexaazatriphenylene
Photocleavage
Polypyridyl

ABSTRACT

This paper describes the synthesis of a trinuclear Cu(II) complex (**4**) containing a central 1,4,5,8,9,12-hexaazatriphenylene-hexacarboxylate (hat) core (**3**). Low, micromolar concentrations of the negatively charged parent ligand **3** and the neutral trinuclear complex **4** were found to photocleave negatively charged pUC19 plasmid DNA with high efficiency at neutral pH (350 nm, 50 min, 22 °C). The interactions of complex **4** with double-helical DNA were studied in detail. Scavenger and colorimetric assays pointed to the formation of Cu(I), superoxide anion radicals, hydrogen peroxide, and hydroxyl radicals during photocleavage reactions. UV–visible absorption, circular dichroism, DNA thermal denaturation, and fluorescence data suggested that the Cu(II) complex contacts double-stranded DNA in an external fashion. The persistent association of ligand **3** and complex **4** with Na(I) and/or other cations in aqueous solution might facilitate electrostatic DNA interactions.

1. Introduction

There is great interest in the design and synthesis of transition-metal complexes that bind to and cleave nucleic acids. Particularly, the study of Ru(II)-complexes based on polypyridyl chelating ligands such as 2,2′-bipyridine (bpy), 1,10-phenanthroline (phen), and 1,4,5,8,9,12-hexaazatriphenylene (hat), have been a major focus of bio-inorganic photochemical research [1–16]. The planar polyazaaromatic ligands of these Ru(II) complexes have the potential to interact with DNA either electrostatically, through intercalation, and/or by surface binding in the DNA grooves [1,3,4,10,14,17]. Because their oxidizing and reducing properties are enhanced in the triplet excited state, substantial levels of photo-oxidative DNA cleavage arise upon irradiation with light [4, 11–16]. This has led to a growing interest in the development of polypyridyl Ru(II)-complexes as photo-therapeutic agents in cancer treatment [13–16]. Photocleavage is thought to entail type 1 electron transfer from the DNA bases to the triplet excited state of the complex [4,11], as well as ground state triplet oxygen ($^3O_2$) dependent processes that involve type 1 superoxide anion radical ($O_2^{\bullet-}$) [16] and/or type 2 singlet oxygen ($^1O_2$) formation [11–16].

While ruthenium and its ions have no known biological functions, copper is essential for maintaining a healthy state in many living organisms, being widely utilized for its redox activity by oxidases and proteins involved in oxygen and electron transport [18]. Moreover, copper(II) ions are closely associated with chromatin [19–21] and play important roles in the regulation of gene expression [18,22,23]. When copper homeostasis is out of balance, normal physiological processes are sometimes altered. High copper concentrations can promote tumor angiogenesis by stimulating endothelial cell proliferation and migration [24–27]. Moreover, elevated tissue and/or serum copper levels have been correlated to tumor occurrence, progression, and recurrence in a wide range of human malignancies including breast, brain, cervical, colorectal, liver, lung, and prostate cancers [25,27–29]. Photosensitizing agents that are activated by copper therefore represent attractive complements to polypyridyl photo-nucleases based on Ru(II) and other metal ion centers. A number of polypyridyl complexes equipped with stable copper cores have shown considerable potential as nucleases for use in photo-therapeutic applications, particularly in the red to near-infrared wavelength range [30–33]. In early, seminal work, Chakravarty and co-workers achieved extremely efficient, type 1 photocleavage of plasmid DNA upon activation of a Cu(II) bis-dipyridoquinoxaline (dpq) photosensitizer at 694 nm (50 μM Cu(II) bis-dpq, 120 min, 22 °C) [31].

In the following report, the negatively charged polydentate hat ligand hexaazatriphenylene-hexacarboxylate (hat-$(COO^-)_6$; **3** in Scheme 1) was shown to produce high levels of DNA photocleavage that were markedly enhanced by addition of Cu(II) (350 nm, 22 °C; pH 7.0). A total of 38 μM bp of supercoiled pUC19 plasmid was completely converted into nicked and linear DNA forms in the presence of sub-micromolar concentrations of **3** and 3 mol equiv of Cu(II). A neutral trinuclear Cu(II) complex based on hat-$(COO^-)_6$ (**3**) was then

* Corresponding authors.
E-mail addresses: antonio.lorente@uah.es (A. Lorente), kbgrant@gsu.edu (K.B. Grant).

http://dx.doi.org/10.1016/j.jinorgbio.2016.12.007
0162-0134/

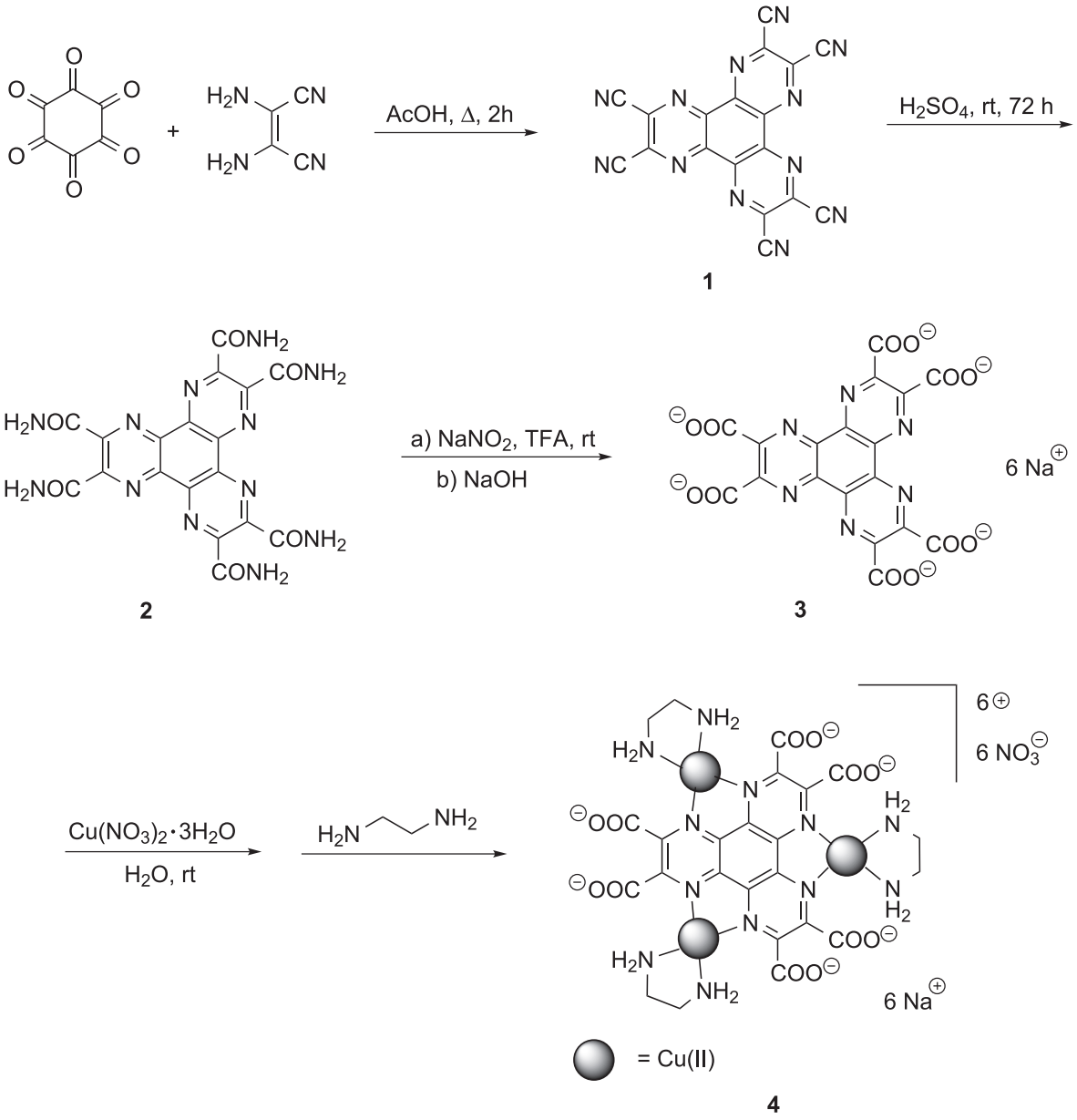

Scheme 1. Synthesis of negatively charged hexaazatriphenylene-hexacarboxylate **3** as a neutral sodium carboxylate salt followed by reaction with copper(II) nitrate trihydrate and ethylenediamine gives the sodium salt of trinuclear Cu(II) complex **4** with a net charge of 6+ and six nitrate counteranions.

synthesized and characterized (($Cu(en))_3$hat-$(COO)_6$; **4** in Scheme 1). Concentrations of the Cu(II) complex as low as 0.5 μM were found to be highly active in DNA photocleavage assays. Spectroscopic data suggested that the external association of **4** with double-helical DNA were likely to have prevailed over intercalative and groove binding modes. The interaction of Na(I) countercations with negatively charged ligand **3**, neutral complex **4**, and negatively charged DNA is discussed.

2. Experimental

2.1. Materials and methods

Distilled, deionized water (ddH_2O) was utilized for the preparation of all buffers and aqueous solutions. Sodium phosphate dibasic salt, sodium phosphate monobasic salt, and ethylenediaminetetraacetic acid disodium salt (EDTA-Na_2) were acquired from Fisher Scientific. Calf thymus (CT) DNA was obtained from Invitrogen (10 mg/mL). pUC19 plasmid DNA was cloned from either XL-1 blue *E. coli* competent cells (Strategene) or DH5-α competent cells according to a standard laboratory procedure [34]. The plasmid DNA was purified with a QIAGEN Plasmid Maxi Kit. Sodium azide ≥99%, bathocuproinedisulfonic acid (BCS) disodium salt hydrate, Chelex® 100 resin, copper(II) chloride dihydrate ≥99%, sodium benzoate 99%, ethidium bromide (EtBr) 99%, catalase from bovine liver, DMSO, 2-[4-(2-hydroxyethyl)piperazin-1-yl]ethanesulfonate sodium salt (HEPES-Na) 99.5%, pentamidine isethionate salt, and superoxide dismutase (SOD) from bovine erythrocytes were acquired from Sigma-Aldrich.

UV–visible spectra were recorded with a UV-2401PC Shimadzu spectrophotometer. CD spectra were acquired using a Jasco J-810 spectropolarimeter. DNA thermal denaturation studies were performed using a Cary 300 Bio UV–visible spectrophotometer fitted with a Cary temperature controller. Fluorescence was measured using a FLUOstar microplate reader equipped with 540 nm excitation and 590 nm emission filters. Photocleavage reactions were run aerobically, with either a low power Esco-Lite UV Ultraviolet LED (light emitting diode) flashlight (390 to 395 nm spectral output) or in a ventilated Rayonet

Photochemical Reactor fitted with ten 24 W RPR-3500 Å lamps (power density per lamp = 9.2 mW cm^{-2} at the center of the reactor; The Southern New England Ultraviolet Company).

2.2. Preparation of trinuclear Cu(II) hexaazatriphenylene-hexacarboxylate complex **4**

The synthesis of the sodium salt of hexaazatriphenylene-hexacarboxylate **3** (hat-$(COO^-)_6$) was accomplished using a previously reported procedure [35]. To a solution of **3** (214 mg, 0.339 mmol) in water (70 mL), copper nitrate trihydrate (246 mg, 1.02 mmol) was added. After that, a dark precipitate was observed, which disappeared upon addition of ethylenediamine (106 mg, 1.752 mmol). The reaction mixture was stirred at room temperature for 96 h, and then the solvent was evaporated under reduced pressure. The resulting residue was treated with absolute ethanol (40 mL) and centrifuged. The solid thus obtained was washed with ethanol (3 × 10 mL) and then dried *in vacuo*, affording as pure product 448 mg (96% yield) of the sodium nitrate salt of **4** ($((Cu(en))_3$hat-$(COO)_6$), mp > 300 °C. IR (KBr): 3310, 3218, 2360, 2341, 1610, 1383, 1043 cm^{-1}. ESI-TOF MS 697.66 $[(M + H + Na)^{2+}$, M = $C_{24}H_{24}Cu_3N_{18}Na_6O_{30}$. Anal. Calcd. for $C_{24}H_{24}Cu_3N_{18}Na_6O_{30}.H_2O$: C, 20.72; H, 1.88; N, 18.12. Found: C, 20.69; H, 2.02; N, 18.60.

2.3. Photocleavage of supercoiled plasmid DNA

In concentration titration experiments, individual DNA samples contained: 0.0 to 5.0 μM of **3** with and without 3 mol equiv of $CuCl_2$ or 0.0 to 20.0 μM of **4**; 38 μM bp pUC19 plasmid; and 10 mM sodium HEPES or sodium phosphate buffer pH 7.0 (40 μL total volume). After a 20 to 60 min equilibration period at room temperature, the solutions were irradiated for 50 min at 350 nm or 395 nm (22 °C).

In time course experiments, 40 μL reactions comprised of 10 mM sodium phosphate buffer pH 7.0 and 38 μM bp of pUC19 plasmid DNA were irradiated in the presence and absence of 2 μM of **4** for 0 min, 10 min, 20 min, 30 min, or 50 min (350 nm, 22 °C). Parallel control reactions containing 2 μM of **4**, 38 μM bp of pUC19, and 10 mM sodium phosphate pH 7.0 were kept in the dark (50 min).

After irradiation, 3 μL of electrophoresis loading buffer (15.0% (w/v) Ficoll, 0.025% (w/v) bromophenol blue) were transferred to each cleavage reaction. Twenty microliter aliquots of the resulting solutions were then loaded onto 1.5% agarose gels stained with ethidium bromide (0.5 μg/mL, final concentration). Electrophoresis was carried out at 160 V using 1× TAE (tris-acetate EDTA) running buffer and an OWL A1 large gel system (Thermo Scientific). Gels were visualized on a trans-illuminator set at 302 nm, photographed, and then quantitated with Image Quant v. 5.0 software. For supercoiled DNA, the numerical values obtained by integrating the pixels within each DNA band were multiplied by a correction factor of 1.22 to account for the decreased affinity of ethidium bromide for supercoiled vs. nicked and linear plasmid forms [36]. Photocleavage yields were then calculated according to the formula:

$$\text{Percent photocleavage} = [(\text{linear or nicked DNA})/(\text{linear} + \text{nicked} + \text{supercoiled DNA})] \times 100.$$

2.4. Colorimetric detection of copper(I)

Individual reactions contained 10 mM of sodium phosphate buffer pH 7.0 and either 10 μM of **4**; 10 μM of **4** and 38 μM bp of calf thymus (CT) DNA; 30 μM of $CuCl_2$; 30 μM of $CuCl_2$ and 38 μM bp of CT DNA, or 38 μM bp CT DNA (600 μL final volume). The samples were gently mixed to avoid shearing the DNA and then incubated at room temperature in the dark for 30 min (22 °C). After this, they were irradiated at 350 nm for 30 min, while a parallel set of negative control reactions was kept in the dark. As a positive control for copper(I) formation, 30 μM of $CuCl_2$ was reacted with one mol equiv of L-ascorbic acid for 30 min at 22 °C. Thereafter, bathocuproinedisulfonic acid disodium salt hydrate (42 μM final concentration) was added, and the reactions were equilibrated in the dark for 30 min at 22 °C. The formation of a 2:1 BCS:Cu(I) complex (λ_{max} = 480 nm) was then monitored by UV–visible spectrophotometry.

2.5. Reagent-induced changes in DNA photocleavage

The following stock solutions were sequentially added to individual Eppendorf® tubes: 100 mM sodium phosphate buffer pH 7.0 (4 μL); neat ddH_2O (0 μL to 30.8 μL) or neat D_2O (31.4 μL); 490.4 μM bp pUC19 plasmid DNA (3.1 μL); and 8 μM (10 μL) or 30.8 μM (1.3 μL) of complex **4** in ddH_2O. Following a brief equilibration period, the solutions were combined with either: 5 μL of 800 U/μL of superoxide dismutase in 100 mM potassium phosphate buffer pH 7.8; 5 μL of 800 U/μL catalase in 50 mM potassium phosphate buffer pH 7.0; 5 μL of 800 mM sodium benzoate in ddH_2O; 5 μL of 800 mM sodium azide in ddH_2O; 0.8 μL DMSO neat; or 8 μL of 500 mM EDTA in ddH_2O (40 μL final volume). The final reagent concentrations in each reaction were: 10 mM sodium phosphate buffer pH 7.0, 38 μM bp pUC19 plasmid DNA, 1 μM or 2 μM of **4**, and either 100 U SOD, 100 U catalase, 100 mM sodium benzoate, 100 mM sodium azide, 79% (v/v) D_2O, 2% (v/v) DMSO, or 100 mM EDTA. Following a brief equilibration period, the reactions were irradiated at 350 nm for 30 min. DNA products were then resolved on 1.5% agarose gels and quantitated as described above. For each reaction, the average reagent-induced % change in DNA photocleavage was calculated from integrated DNA band intensities using the formula:

$$\text{Percent photocleavage change } (\%) = [(\%\text{total of linear and nicked DNA}_{\text{without reagent}} - \%\text{total of linear and nicked DNA}_{\text{with reagent}})/(\%\text{total of linear and nicked DNA}_{\text{without reagent}})] \times 100.$$

2.6. Circular dichroism

Solutions for CD analysis contained 10 mM of sodium phosphate buffer pH 7.0 in the presence and absence of 150 μM bp of CT DNA and 8 to 91 μM of complex **4**. After a 60 min pre-equilibration period (22 °C, no hν), spectra were collected from 400 to 190 nm in 1 mL (0.2 cm) quartz cuvettes (Starna) with a response time of 1 s and a scan rate of 100 nm/min. The sensitivity was 100 millidegrees and the bandwidth was set at 2 nm. Final spectra were averaged over 16 acquisitions.

2.7. Thermal denaturation experiments

Individual solutions containing 10 mM sodium phosphate buffer pH 7.0 and 19 μM bp of CT DNA in the presence or absence of either 1 μM **4** or 3 μM $CuCl_2$ were transferred to a 1.5 mL Starna quartz cuvette (1 cm) and allowed to equilibrate for 15 min at 22 °C. Absorbance was then monitored at 260 nm as the temperature was increased from 25 °C to 100 °C at a rate of 0.5 °C min^{-1}. The first-derivative of $\Delta A_{260}/\Delta T$ (y) versus temperature (x) was calculated using KaleidaGraph software v. 4.0. The maximum of each resulting first-derivative plot was then identified with the KaleidaGraph Gaussian curve fit function y = m1 + m2 * e(−(x − m3)^2/m4^2), where m3 is the temperature at the estimated maximum value of y.

2.8. Fluorescence quenching experiments

Solutions containing EtBr and sodium phosphate buffer pH 7.0 were pre-equilibrated in the absence and presence of CT DNA for 30 min at room temperature. Fifty microliter aliquots of each solution were

transferred to the wells of a white Corning 96-well non-binding polystyrene microplate. This was followed by the addition 0.125 to 45 μL of a 100 μM stock solution of a potential quenching agent (either EDTA, $CuCl_2$, pentamidine, or complex **4**) followed by ddH_2O to a final volume of 100 μL per well. Each well contained 12 μM of EtBr, 19 μM bp of CT DNA, 10 mM of sodium phosphate buffer, and 0.125 μM to 45 μM of quencher. In a second set of experiments, to the microplate wells containing CT DNA, EtBr, and sodium phosphate buffer were added 2 to 14 μL aliquots of a 3 mM quencher stock solution followed by ddH_2O to a final volume of 100 μL. The wells contained 12 μM of EtBr, 19 μM bp of CT DNA, 10 mM of sodium phosphate buffer, and 60 μM to 420 μM of quenching agent. After a 15 min equilibration period at room temperature, microplates were excited at 540 nm and read for fluorescence at 590 nm against blanks containing 10 mM sodium phosphate buffer pH 7.0.

Relative fluorescence intensities of individual wells were calculated according to fluorescence generated by standard solutions containing 12 μM ethidium bromide, 19 μM bp of CT DNA, and 10 mM sodium phosphate buffer pH 7.0 as follows:

Relative fluorescence intensity
= (fluorescence of sample well/fluorescence of standard well) × 100.

The relative fluorescence intensity data were plotted as a function of increasing quencher concentration and then curve fit using IGOR Pro 6.34 (WaveMetrics, Inc.) to the linear ($I_o/I = 1 + K_{SV}[Q]$; [37]) and quadratic ($I_o/I = (1 + K_D[Q])(1 + K_S[Q])$; [38,39]) forms of the Stern-Volmer equation. I_o = EtBr fluorescence intensity without quencher; I = EtBr fluorescence intensity with quencher; K_{SV} = Stern-Volmer quenching constant; K_D = dynamic quenching constant; K_S = static quenching constant; [Q] = quencher concentration.

3. Results and discussion

3.1. Metal activated DNA photocleavage by hat-$(COO^-)_6$ (**3**)

The elevated tissue and/or serum copper levels that occur in a wide range of human malignancies suggest that DNA photo-nucleases with the potential to be triggered by copper ions might show promise as selective anti-cancer photo-therapeutic agents [25,27–29]. For this study, we chose the polypyridyl, π acceptor ligand hat-$(COO^-)_6$ (**3**) as a potential, copper-activatable DNA photosensitizer for the following reasons [35]. The high excited state reduction potential of a ruthenium(II) complex of hat ($Ru(hat)_3^{2+}$; $E^*_{red} = +1.49$ V) causes the complex to be highly oxidizing in its excited state [11]. As a result, $Ru(hat)_3^{2+}$ generates efficient photo-oxidative cleavage of plasmid DNA when compared to non-oxidizing polypyridyl analogs such as $Ru(phen)_3^{2+}$ and $Ru(bpy)_3^{2+}$ ($E^*_{red} = +0.70$ V and $+0.65$ V, respectively) [11]. The ground state reduction potentials of the Cu(II)/Cu(I) couple of typical Cu(II) polypyridyl complexes range from −0.1 V to +0.09 [30–32], and thus are significantly higher when compared the ground state Ru(II)/Ru(I) couple even in highly oxidizing Ru(II) complexes ($E_{red} = -0.82$ V to -0.62 V) [11]. Moreover, hat is capable of forming stable mononuclear and polynuclear Cu(II) coordination compounds [40–42]. With the above being said, we hypothesized that any copper(II) ions sequestered by this ligand in cancer cells might undergo facile, excited state one electron photo-reduction. The copper(I) centers thus formed would be expected to transfer electrons to $^3O_2$ to generate $O_2^{\bullet-}$ followed by highly reactive, DNA damaging hydroxyl radicals [31,43–46].

The hat-$(COO^-)_6$ ligand **3** was synthesized as the sodium salt (hat-$(COONa)_6$) according to the series of reactions shown in Scheme 1. The six carboxylate units were incorporated into the design of **3** in order to increase water solubility and, upon water solvation of the sodium counter cations of (hat-$(COONa)_6$), to impart negative charge that would minimize background interactions between **3** (hat-$(COO^-)_6$) and negatively charged DNA.

In our first set of photocleavage experiments, pUC19 plasmid DNA was equilibrated with increasing concentrations of hat-$(COO^-)_6$ (**3**) in the presence and absence of 3 mol equiv of $CuCl_2$ (10 mM HEPES buffer pH 7.0; 22 °C for 60 min). The samples were then irradiated for 50 min at 350 nm and resolved on agarose gels. The conversion of supercoiled plasmid to nicked and linear DNA forms was visualized by ethidium bromide staining. High levels of DNA cleavage at extremely low molar ratios (**r**) of hat-$(COO^-)_6$ to DNA were observed, where **r** = [**3**]/[DNA bp] (Fig. 1A). With the exception of one ligand concentration (1.0 μM of **3**), DNA damage was markedly increased upon the addition of 3 mol equiv of copper(II) (0.1 μM, 0.5 μM, and 5.0 μM of **3**; Lanes 1 vs. 5, 2 vs. 6, and 4 vs. 8 in Fig. 1A, respectively). The control reactions in Fig. S1 show that the combination of hat-$(COO^-)_6$ and light was required for cleavage to occur. Very little DNA damage was observed in "copper only" and "dark" controls in which **3** or light were respectively omitted (Fig. S1 in Supplementary data). Three mol equiv of Cu(II) did not increase DNA photocleavage in the case of 1.0 μM of **3**, presumably due to experimental error and/or possible competition between Cu(II) ions and **3** for binding sites on DNA (lanes 3 vs. 7 in Fig. 1A) [47].

While addition of Cu(II) increased DNA cleavage markedly, irradiation of sub-micromolar to micromolar concentrations of hat-$(COO^-)_6$ unexpectedly generated significant amounts of background DNA degradation (no Cu(II); Lanes 5 to 8 in Fig. 1A). The two carboxylate groups of the hat-$(COO^-)_6$ analog 2,3-pyrazinedicarboxylic acid possess pK_a values of 2.77 and 4.06 [48], suggesting that, upon water solvation of the six Na(I) countercations of the synthesized sodium salt hat-$(COONa)_6$ (Scheme 1), hat ligand **3** would be negatively charged at a pH value of 7.0. This would in turn be predicted to hinder its association with negatively charged duplex DNA under the pH 7.0 reaction conditions used in the cleavage experiment (Fig. 1A). Nonetheless, the significant photo-damage produced by hat-$(COO^-)_6$ in the absence of added

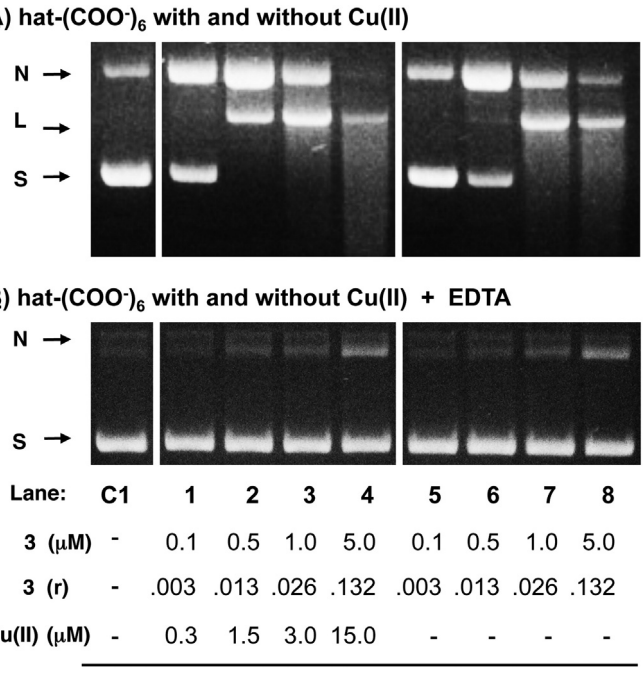

Fig. 1. Photograph of 1.5% agarose gels showing DNA photocleavage in the absence (A) and presence (B) of 25 mM of EDTA. Reactions containing 38 μM bp of pUC19 and 0, 0.1, 0.5, 1.0, and 5.0 μM of hat-$(COONa)_6$ (**3**) in the absence and presence of 3 mol equiv of $CuCl_2$ were irradiated in an aerobically ventilated Rayonet Photochemical Reactor containing ten RPR-3500 Å lamps (50 min and 22 °C; 10 mM HEPES buffer pH 7.0; power density per lamp ≈ 9.2 mWcm^{-2}). In lanes 3, 4, 7, and 8 of (A), plasmid was degraded into diffuse bands of high mobility DNA fragments. C1 = light only DNA control (no **3** or Cu(II)). Abbreviations: **L** = linear; **N** = nicked; **S** = supercoiled; **r** = **3** to DNA bp molar ratio = [**3**]/[DNA bp].

Cu(II) indicated that ligand **3** was in close enough proximity to DNA to photosensitize direct cleavage of the nucleic acid (*e.g.*, by type 1 electron transfer and/or type 2 energy transfer to diffusible $^3O_2$; Fig. 1A).

A possible factor contributing to DNA photocleavage by negatively charged hat-$(COO^-)_6$ (**3**) is the general propensity of carboxylate and phosphate groups to associate with sodium(I) cations in water. Published stability constants for a number of carboxylate ligands (*e.g.*, log $\beta_{Na\text{-}L} = 2.36 \pm 0.03$ for benzenehexacarboxylic acid) confirm that carboxylates form weak ionic complexes with Na(I) in aqueous solution [49]. Molecular dynamics simulations suggest that these interactions involve the formation of both direct [50,51] and water-mediated [52] ion pairs between carboxylate anions and the sodium cations. It is therefore possible that hat-$(COO^-)_6$ (**3**) retained an ability to interact with Na(I) during the photocleavage experiment in Fig. 1A (*e.g.*, via hat-$(COONa)_6$). The metal ion source could have been the six original sodium(I) countercations used to synthesize the sodium salt of **3** or sodium ions from the photocleavage reaction buffer (10 mM HEPES-Na pH 7.0).

In addition to carboxylates, the negatively charged phosphate groups of DNA attract sodium ions in aqueous environments [53–57]. Sodium(I) and other cations are predicted to form a mobile ion atmosphere that neutralizes the opposing negatively charged phosphate groups in the backbone of each DNA strand, allowing the DNA helix to form [53,55–57]. In the case of Na(I), the ion atmosphere has been quantitated by atomic emission spectroscopy and small-angle X-ray scattering (SAXS) experiments, showing that the number of sodium atoms is directly related to the number of phosphate groups in the DNA [55,57]. Molecular dynamic simulations point to the formation of short-lived, diffusible ion pairs between Na(I) and the phosphate groups [54]. According to Monte Carlo simulations, the Na(I) atmosphere extends out from DNA by approximately 7 Å [53]. If the Na(I) counterions associated with hat-$(COO^-)_6$ (**3**) were to become absorbed into such an ion atmosphere, then a templating effect might be induced in which **3** would be brought in close enough proximity to DNA for photocleavage to occur. A second possible explanation to account for hat-$(COO^-)_6$-DNA interactions at pH 7.0 could involve chelation of adventitious, redox active trace metal ions (*e.g.*, Cu(II) and Fe(III)) by the six nitrogen donor atoms of hat. This would add positive charge to the ligand, allowing hat-$(COO^-)_6$ (**3**) (or hat-$(COONa)_6$) to associate with DNA electrostatically. Direct DNA strand breaks could then be photosensitized upon irradiation with ultraviolet light.

In order to evaluate the preceding hypotheses, the photocleavage experiment shown in Fig. 1A was repeated in the presence of excess EDTA, a metal chelating agent that interacts with Na(I) (log $\beta_{Na\text{-}EDTA} = 2.04 \pm 0.04$) and to a much greater extent, the redox active ions Cu(II) and Fe(III) (log $\beta_{M\text{-}EDTA} = 18.8$ and 25.1 ± 0.05, respectively) [58]. In the hat-$(COO^-)_6$ (**3**) reactions run with and without 3 mol equiv of exogenous copper(II), DNA damage was markedly inhibited by EDTA, pointing to the participation of metal ions in both sets of reactions (Fig. 1B). As a further test for metal ion involvement, we attempted to reduce hat-$(COO^-)_6$ (**3**) background cleavage (no exogenously added copper(II)) by pre-treating ddH_2O and the pH 7.0 photocleavage reaction buffer with Chelex® 100 resin, a styrene divinylbenzene copolymer modified with metal chelating iminodiacetate groups. Chelex® 100 resin displays strong selectivity for removing copper, iron, and other transition metal ions from laboratory solutions over monovalent cations such as sodium(I) and potassium(I) [59]. However, Chelex® treatment of the ddH_2O and reaction buffer had no effect on DNA cleavage yields (Fig. S2 in Supplementary data). This suggested to us that hat-$(COO\text{-})_6$ was persistently associating with sodium(I) countercations in the photocleavage reaction, allowing DNA interactions to occur. Since transition metal ions were not involved in the synthesis of sodium salt hat-$(COONa)_6$ (Scheme 1) [35], we also considered the possibility that the plasmid DNA preparation used in our photocleavage experiments might have contained trace levels of adventitious transition metals that were being sequestered by the hat ligand, facilitating its association with DNA. *In vitro*, Cu(II) is known to bind to negatively charged oxygen atoms in the DNA phosphate backbone and with nitrogen and oxygen donor atoms located in guanine and cytosine bases [60]. Moreover, the presence of trace metals in nucleic acid preparations has been confirmed experimentally. In studies that have systematically determined metal content, DNA and RNA samples isolated by conventional laboratory methods have been found to contain adventitious copper(II) and other redox active metal ions directly bound to the nucleic acids [19, 60–64].

3.2. DNA photocleavage by trinuclear Cu(II) hat-$(COO\text{-})_6$ complex **4**

In order to minimize possible interference arising from adventitious transition metals and to better understand the specific roles played by copper(II) in hat-$(COO^-)_6$-sensitized DNA photocleavage, the trinuclear Cu(II) complex $(Cu(en))_3$hat-$(COO)_6$ (**4**) was prepared (Scheme 1). Ethylenediamine (en) was incorporated into **4** as an ancillary ligand to prevent the formation of extended hat-$(COO)_6^-$ copper(II) coordination polymers [42]. The synthesis of **4** as the sodium nitrate salt $[(Cu(en))_3$hat-$(COONa)_6](NO_3)_6$ was then accomplished by adding three equiv of copper nitrate trihydrate to an aqueous solution of sodium hexaazatriphenylene-hexacarboxylate at room temperature, followed by the addition of 5 mol equiv of en.

In order to evaluate trinuclear Cu(II) complex **4** for DNA photocleaving activity, a preliminary concentration profile was carried out. Individual reactions consisted of 0 μM to 2 μM of **4** and 38 μM bp pUC19 plasmid DNA in 10 mM sodium phosphate buffer pH 7.0. The samples were irradiated for 50 min at 350 nm and 22 °C and then resolved on a 1.5% agarose gel (Fig. 2). The results of the profile revealed high levels of DNA photocleavage at extremely low molar ratios (**r**) of the complex to DNA, where **r** = [**4**]/[DNA bp]. After 50 min of irradiation, almost all of the supercoiled plasmid was converted into nicked and linear DNA product in the presence of 1 μM (**r** = 0.026; 84% nicked and 14% linear) and 2 μM (**r** = 0.053; 66% nicked and 33% linear) concentrations of complex **4** (Lanes 5 and 6 in Fig. 2). In the absence of the complex, little if any DNA photocleavage was observed (Lane 1 in Fig. 2).

In our next experiment, individual reactions containing 38 μM bp of pUC19 plasmid DNA and 2 μM of **4** were irradiated at time intervals

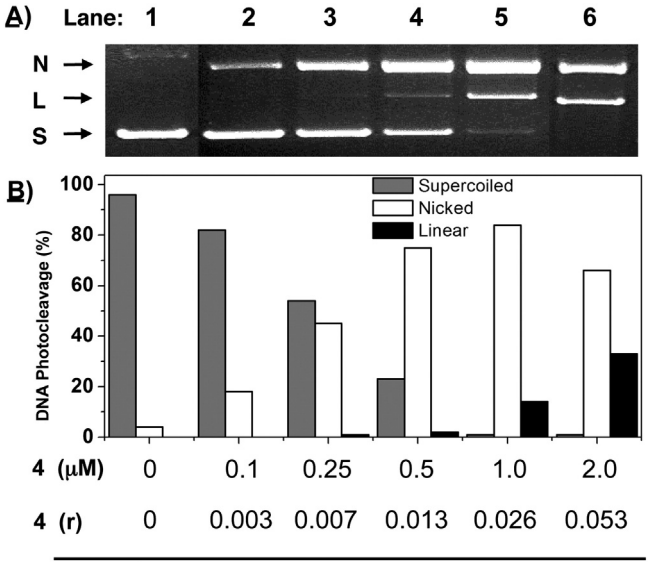

Fig. 2. A 1.5% agarose gel (A) and corresponding histogram (B) showing photocleavage of 38 μM bp pUC19 DNA by 0, 0.1, 0.25, 0.5, 1.0, and 2.0 μM of **4** (10 mM sodium phosphate buffer pH 7.0). Reactions were irradiated in an aerobically ventilated Rayonet Photochemical Reactor containing ten RPR-3500 Å lamps (50 min, 22 °C; power density per lamp ≈ 9.2 mW cm^{-2}). Abbreviations: **L** = linear; **N** = nicked; **S** = supercoiled; **r** = complex **4** to DNA bp molar ratio = [complex]/[DNA bp].

ranging from 0 to 50 min (350 nm, 22 °C). The data in Figs. 3 and S3 reveal the formation of photocleaved DNA product after 10 min of irradiation (5% linear and 70% nicked). At the 30 min time point, the plasmid DNA was cut in 96% yield. Between 30 and 50 min, a decrease in the amount of nicked DNA (78% to 66%) gave rise to a corresponding increase in linear DNA product (18% to 33%). DNA cleavage levels were extremely low in "light only" and "dark" control reactions in which complex **4** and light were respectively omitted (Lanes 1 and 2 in Fig. S3).

Upon water solvation of $[(Cu(en))_3hat\text{-}(COONa)_6](NO_3)_6$, the synthesized sodium nitrate salt of **4** (Scheme 1), free $(Cu(en))_3hat\text{-}(COO)_6$ complex (**4**) would be expected to be near neutral in charge at pH 7.0. A relatively weak affinity for negatively charged duplex DNA would therefore be anticipated. However, the strong DNA photocleavage exhibited by low, micromolar concentrations of **4** (Figs. 2, 3, and S3) points to close interactions with DNA. In a similar fashion to **3** (hat-$(COO\text{-})_6$), it is possible that the carboxylate groups of complex **4** are capable of weakly associating with Na(I) ions, either from bulk solution and/or from the ion atmosphere surrounding DNA. This could conceivably add positive charge to the complex, enabling **4** to electrostatically interact with the DNA duplex [49–53,55–57].

3.3. Colorimetric detection of copper(I)

Taking into account the well-documented involvement of copper(II) ions in oxidative stress and redox cycling reactions, our next goal was to obtain experimental evidence that might substantiate a photo-induced DNA cleavage process involving the copper(II) reduction [31,43–46]. We utilized a colorimetric assay based on bathocuproinedisulfonic acid (BCS) disodium salt hydrate, which forms a 2:1, orange-colored complex with Cu(I) ($\lambda_{max} = 480$ nm; $\varepsilon = 13.500\ M^{-1}\ cm^{-1}$) [43–45,65]. Individual samples consisted of either 10 μM of $(Cu(en))_3hat\text{-}(COO)_6$ (**4**) or 30 μM of $CuCl_2$ in the presence or absence of 38 μM bp calf thymus (CT) DNA. After an initial 30 min equilibration period, the samples were irradiated for 30 min at 350 nm. BCS was then added, and the samples were analyzed by UV–visible spectrophotometry. As a positive control for Cu(I) formation, BSC was equilibrated with 30 μM of $CuCl_2$ in the presence of the reducing agent L-ascorbic acid (no hν, Fig. 4A).

As expected, the addition of BCS to the $CuCl_2$/L-ascorbic acid control produced a bright orange signature 480 nm absorption band corresponding to the Cu(I)-BCS complex (Fig. 4A) [65]. Upon irradiation at 350 nm, strong and intermediate Cu(I) signals were respectively generated when CT DNA, 10 μM of trinuclear Cu(II) complex **4** and 30 μM of

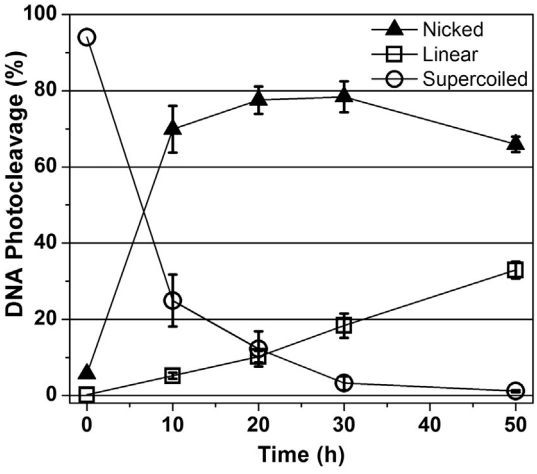

Fig. 3. Photocleavage of 38 μM bp of pUC19 plasmid DNA by 2 μM of complex **4** irradiated at 22 °C for 0, 10, 20, 30, and 50 min time intervals (350 nm with ten lamps, power density per lamp ≈ 9.2 mW cm^{-2}; 10 mM sodium phosphate buffer pH 7.0). Data are averaged over three trials and error bars represent standard deviation. A representative time course gel is shown in Fig. S3.

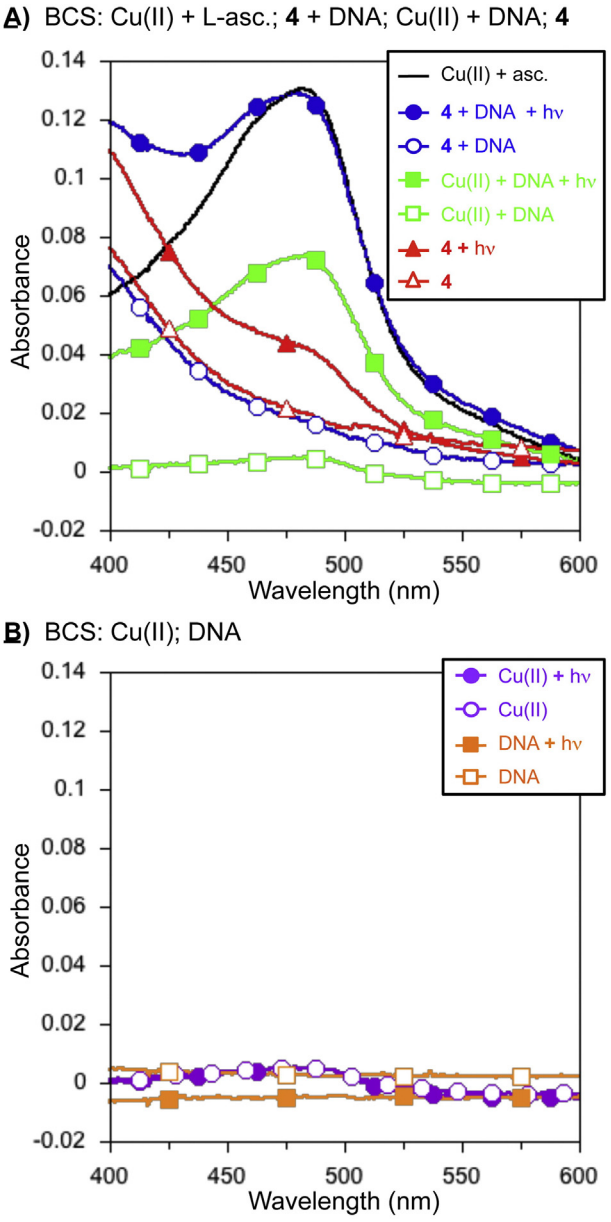

Fig. 4. UV–visible absorption spectra to detect Cu(I)-BCS complex formation (10 mM sodium phosphate buffer pH 7.0). Reactions containing one or more of the following reagents were irradiated at 350 nm (hν) or kept in the dark: 30 μM of $CuCl_2$; 30 μM L-ascorbic acid; 10 μM of **4**; 38 μM bp CT DNA. After 30 min, BCS (42 μM final concentration) was added, and the reactions were equilibrated for an additional 30 min prior to recording the UV–visible spectra (22 °C).

$CuCl_2$ were present in combination. In contrast, a relatively weak Cu(I) signal was observed when 10 μM of complex **4** was unaccompanied by DNA (30 min at 350 nm, Fig. 4A). With six electron withdrawing carboxylate groups, the π-system of central hat-$(COO^-)_6$ ligand of complex **4** is electron deficient [42]. Taken together with the BCS data, this suggests that DNA might be a better donor of electrons to copper(II) than the hat-$(COO^-)_6$ ligand of the complex (Fig. 4A). Copper(I) BCS signals were not seen in irradiated reactions containing either Cu(II) or DNA alone (Fig. 4B) as well as in dark control reactions (dashed lines in Fig. 4) or in reactions in which BCS was omitted (Fig. S4 in Supplementary data).

The BCS results clearly indicate that DNA is independently capable of sensitizing the one electron photo-reduction of Cu(II) to Cu(I). The Rayonet RPR-3500 Å lamps that were used in the preceding photocleavage experiments have a bell-shaped spectral distribution

that ranges from approximately 290 nm to 410 nm with a maximum output value at 350 nm. While copper(II) chloride absorbs poorly in this region, there is major overlap between the lamp output and the absorption spectrum of complex **4** ($\lambda_{max} = 323$ nm) and slight overlap with the absorption spectrum of DNA ($\lambda_{max} = 259$ nm; Fig. S5). Rongoni and co-workers used Cu-K-Edge X-ray absorption spectroscopy to monitor the oxidation states of copper ions directly bound to DNA. When CT DNA samples were pre-equilibrated with $CuCl_2$ and then irradiated at 310 nm, the authors demonstrated that approximately 35% of DNA-bound copper was reduced to copper(I) as a result of one-electron transfer from DNA to copper(II) [62].

The photo-reduction of Cu(II) can be viewed in the context of DNA photocleavage yields. As stated, when 38 μM bp of DNA was present in reactions, irradiating 30 μM of $CuCl_2$ and 10 μM of complex **4** generated intermediate and high levels of copper(I) respectively (Fig. 4A). By comparison, 30 μM of $CuCl_2$ produced extremely low levels of DNA photo-damage (Fig. S6) compared to 2 μM of complex **4**, which caused near-complete DNA degradation (Figs. 2, 3, and S3). The apparent dissociation constant reported for the major Cu(II) binding site in double-helical DNA is in the micromolar range [47], suggesting that copper ions were directly bound to DNA in the BCS and photocleavage experiments that employed $CuCl_2$ (Figs. 4A and S6). In the presence of ground state triplet oxygen ($^3O_2$), the reduction of Cu(II) to Cu(I) generates DNA cleaving reactive oxygen species (ROS), either free hydroxyl radicals (•OH) [31,43–46] (as in a Cu(I)-based Fenton-type reaction) or Cu(I)-peroxides [65–68]. If copper(I) had played a role in ROS production and DNA photocleavage in our experiments, then it might have done so in an inefficient fashion when bound directly to DNA. The hat-$(COO\text{-})_6$ ligand of complex **4** is clearly instrumental in photosensitizing DNA damage.

When the high intensity broad spectrum 290 nm to 410 nm RPR-3500 Å Rayonet lamps used the photocleavage experiments were replaced with a low intensity 390 to 395 nm LED flashlight, complex **4** was still capable of generating DNA photocleavage (Fig. S7). The LED excitation wavelengths were well outside of the range of DNA absorption (Fig. S5), showing that direct excitation of DNA by light is not required for complex **4** to photosensitize DNA damage.

3.4. Reagent-induced changes in DNA photocleavage

The effects of enzymatic and chemical reagents on the DNA photocleaving activity of $(Cu(en))_3$hat-$(COO)_6$ (**4**) were studied next. Separate reactions consisting of 38 μM bp of pUC19 plasmid and 1 μM to 2 μM of **4** were pre-equilibrated with either the singlet oxygen ($^1O_2$) scavenger sodium azide, the hydroxyl radical (•OH) scavengers sodium benzoate and DMSO, the hydrogen peroxide (H_2O_2) scavenger catalase, the superoxide anion radical ($O_2^{\bullet-}$) scavenger superoxide dismutase (SOD), EDTA, and D_2O. Out of all of the reagents tested, the most significant effect on DNA photocleavage was exhibited by EDTA. Single- and double-strand break formation was almost completely prevented by the metal chelator (Table 1, Fig. S8). UV–visible spectra were then recorded upon the addition of EDTA to an aqueous solution of $(Cu(en))_3$hat-$(COO)_6$ (**4**). The optical properties of the complex were markedly altered as a result. A broad 425 nm to 475 nm shoulder absent in the case of hat-$(COO^-)_6$ (**3**), but present for $(Cu(en))_3$hat-$(COO)_6$ (**4**) was reduced in intensity (Fig. S9 in Supplementary data). While it is possible that EDTA also diminished weak interactions between Na(I) ions and carboxylate groups of **4**, the spectral changes illustrated in Fig. S9 suggest that photocleavage inhibition by EDTA involves an interaction between the chelating agent and the copper(II) centers of **4**.

Table 1
Average % change in DNA photocleavage induced by scavengers, D_2O, and EDTA.

Reagent	Species targeted	Photocleavage change (%)[a]
EDTA	Cu(II)	−90 ± 2
Sodium azide	$^1O_2$	−89 ± 2
DMSO	•OH	−71 ± 7
Catalase	H_2O_2	−69 ± 3
Sodium benzoate	•OH	−58 ± 8
SOD	$O_2^{\bullet-}$	−39 ± 2
D_2O	$^1O_2$	−5 ± 1

[a] Data are averaged over three trials and error is reported as standard deviation. Photocleavage gels appear in Supplementary data (Figs. S8 and S10).

The singlet oxygen ($^1O_2$) scavenger sodium azide also exhibited a strong inhibitory effect on DNA photocleavage. Polypyridyl complexes based on copper(II) and other metal ions are capable of photosensitizing the production of DNA damaging singlet oxygen through a type 2 energy transfer pathway [11–16,31,32]. While alkaline- and piperidine labile lesions at guanine bases are the most commonly observed reaction products, singlet oxygen also generates direct DNA strand breaks. Experiments conducted in the presence of the singlet oxygen scavenger sodium azide and D_2O, a solvent that increases the lifetime of singlet oxygen, have shown that $^1O_2$ forms direct strand breaks at guanines under neutral to near-neutral reaction conditions (pH 7.0 to 7.4), without requiring subsequent treatment with a base to induce the cleavage [30,32,33,36,69–72]. This being said, we used D_2O in an attempt to confirm $^1O_2$ involvement in our reactions. However, replacing ddH_2O with the D_2O failed to enhance complex **4**-sensitized photocleavage yields (Table 1, Fig. S10). This pointed to the possibility that a scavenging reaction between sodium azide and singlet oxygen had never occurred. Taking into consideration that azide can serve as a copper binding ligand in aqueous solution [73,74], the D_2O data suggest that the DNA photocleavage inhibition displayed by sodium azide may have arisen from a disruptive interaction between azide anions and the copper(II) centers of **4**.

Inhibition by DMSO, sodium benzoate, catalase, and SOD, respectively indicates that hydroxyl radicals, hydrogen peroxide, and superoxide anion radicals participate in complex **4** sensitized DNA photocleavage (Table 1; Figs. S8 and S10). While hydrogen peroxide and superoxide anion radicals are relatively unreactive towards nucleic acids [75], hydroxyl radicals are powerful biological oxidants that produce direct DNA strand breaks by abstracting hydrogen atoms from deoxyribose [75,76]. The reaction of ground state triplet oxygen with copper(I) has been shown to trigger Cu(II)/Cu(I) redox cycling and DNA cleavage involving the formation of superoxide anion radicals [43–45], hydrogen peroxide [44], and hydroxyl radicals [43,44,46]. It is therefore conceivable that the hydroxyl radicals responsible for DNA cleavage in our experiments are generated by a process similar to the series of reactions shown in Fig. 5. It is possible to consider a scenario in which photo-assisted electron transfer from DNA to complex **4** reduces Cu(II) to Cu(I). The Cu(I) then reacts with ground state triplet oxygen to produce superoxide anion radicals that undergo spontaneous dismutation to form hydrogen peroxide [45]. Hydroxyl radicals, hydroxide anions, and Cu(II) could subsequently be produced via a Fenton-type reaction.

3.5. DNA binding mode analyses

3.5.1. UV–visible spectrophotometry

In order to identify additional factors contributing to the high levels of DNA photocleavage produced by $(Cu(en))_3$hat-$(COO)_6$ (complex **4**), a series of binding mode studies was undertaken. Polypyridyl complexes are known to interact with DNA either electrostatically, through

$$Cu(I) + O_2 \longrightarrow Cu(II) + O_2^{\bullet-}$$

$$2O_2^{\bullet-} + 2H^+ \longrightarrow H_2O_2 + O_2$$

$$Cu(I) + H_2O_2 \longrightarrow HO^{\bullet} + HO^- + Cu(II)$$

Fig. 5. Proposed mechanism for ROS production by copper(I).

intercalation, and/or by surface binding in the DNA grooves [1,3,4,10,14,17,77]. In the case of intercalative binding, electronic effects involving π-π stacking with DNA base pairs produce significant hypochromism and red-shifting in the absorption spectra of the complexes [1,3,17]. Because the strength of electronic interactions is inversely proportional to the cube of the distance separating a given chromophore from the DNA bases [78], DNA-induced changes in absorption are intermediate for groove binding compounds [1] and weakest in the case of complexes that associate with DNA by external electrostatic interactions [1,17,77,79]. UV–visible spectrophotometry was therefore utilized as an initial method to investigate DNA binding. Fig. 6 shows the absorption spectra recorded for solutions containing 8 μM of complex **4** and 38 μM bp CT DNA alone and in combination. While datapoints from 200 nm up to approximately 310 nm were difficult to evaluate due to strong, overlapping absorption by **4** and DNA, the complex **4** absorption maximum at 323 nm was unaffected by DNA addition at a complex to DNA bp molar ratio (**r**) equal to 0.211 (Fig. 6). Bathochromic and hypochromic changes to the 323 nm absorption band could not be detected even after the CT DNA concentration was incrementally increased from 38 up to 304 μM bp (Fig. S11). Interestingly, the molar ratios in these UV–visible experiment overlap with the range of **r** values that produces DNA photocleavage (**r** = 0.211 to 0.026 in Fig. S11 vs. **r** = 0.053 to 0.003 in Fig. 2).

Putting the preceding DNA bp molar ratios into context, published DNA titration experiments have shown that the UV–visible spectra of typical DNA binding ligands are altered upon DNA addition over broad **r** value ranges, with the tighter binding compounds generally requiring less DNA to induce detectable spectral changes (*e.g.,* **r** = 2.5 to 0.833, $K_{app} = 7.48 \times 10^3\ M^{-1}$; **r** = 5.0 to 0.833, $K_{app} = 4.49 \times 10^4\ M^{-1}$; **r** = 5.0 to 0.417, $K_{app} = 3.77 \times 10^5\ M^{-1}$; **r** = 10.0 to 1.0, $K_{app} = 1.24 \times 10^6\ M^{-1}$) [80–83]. Although uncommon, it is important to note that an absence of DNA-induced variations in chromophore absorption has been reported in the case of positively charged polypyridyl complexes that associate with DNA predominantly by electrostatic interactions [1,17]. Complex **4** is clearly capable of sensitizing DNA photocleavage at low, micromolar concentrations of complex (Figs. 2, 3, S3, and S7). The scavenger experiments in Table 1 show that short-lived hydroxyl radicals are likely to be generated (Fig. 5). Hydroxyl radicals have a diffusion radius of approximately 20 Å and therefore must be produced in close proximity to DNA for cleavage to occur [84]. While complex $(Cu(en))_3$hat-$(COO)_6$ (**4**) would be expected to be near neutral in charge at pH 7.0, a persistent weak association of the carboxylate groups of the complex with Na(I) ions from bulk solution and/or from the ion atmosphere of DNA could conceivably increase positive charge and facilitate electrostatic DNA interactions [49–53,55–57].

3.5.2. Circular dichroism spectroscopy

A series of circular dichroism (CD) spectra was recorded in our next set of experiments. Upon binding to DNA by intercalation or within the DNA grooves, achiral chromophores generate induced circular dichroism (ICD) signals in the spectra of the chiral nucleic acid helix [85]. In addition to producing ICDs, most intercalators reduce the helical twist angle of the DNA, resulting in a pronounced reduction in the intensity of the positive DNA CD signal at 280 nm [36,86]. In contrast to intercalating and groove binding agents, compounds that associate with DNA primarily by external, electrostatic interactions generally do not generate ICDs or make major changes to the DNA CD spectrum [17,77,79,87]. As shown in Fig. 7, the CD signal of CT DNA is nearly superimposable with all of the spectra acquired upon subsequent addition of increasing concentrations of **4**. While CD measurements at high **r** values (≥0.41) exhibited extremely subtle spectral changes, induced CD signals corresponding to complex **4** could not be resolved even at the highest **r** value tested (**r** = 0.61 in Fig. 7). The CD data taken together with the UV–visible absorption and photocleavage results suggest that **4** is unlikely to be binding to DNA through traditional intercalative or surface-groove modes, but instead may be engaging in external interactions.

3.5.3. Thermal melting experiments

In general, intercalation stabilizes double-helical DNA, producing relatively large enhancements in DNA melting temperature (T_m), the point at which half of the DNA duplex is denatured to a single-stranded state [1,3,88,89]. In the case of polypyridyl complexes that interact with DNA by intercalation, 4 °C to 5 °C increases in DNA T_m have been reported [1,88]. In contrast, T_m enhancements are smaller in the case of compounds that associate with DNA either electrostatically [1,89] or through surface-groove interactions [88]. When recorded under

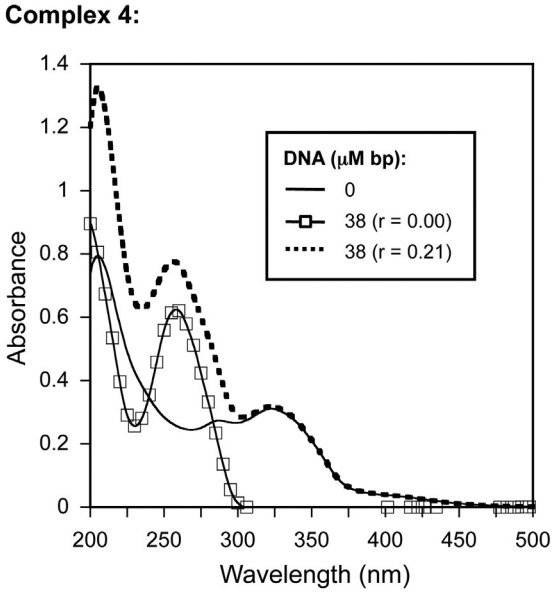

Fig. 6. UV–visible absorption spectra of: 8 μM of **4** (solid line); 38 μM bp of CT DNA (boxes); and 8 μM of **4** in the presence of 38 μM bp of CT DNA (dashed line) recorded in 10 mM sodium phosphate buffer pH 7.0. Absorption spectra were corrected for sample dilution. Abbreviation: **r** = complex **4** to DNA bp molar ratio = [complex]/[DNA bp].

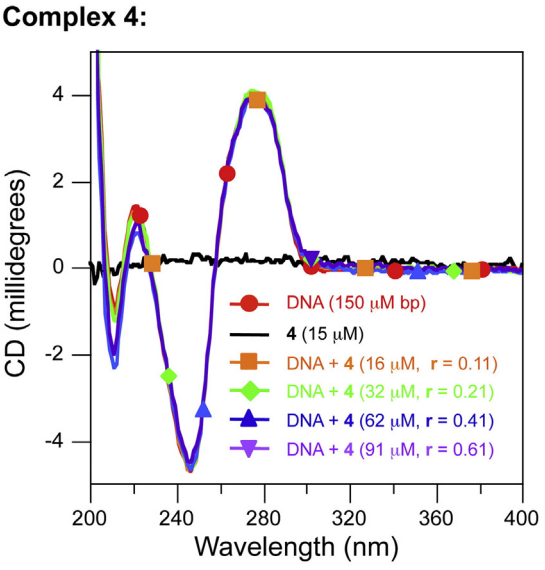

Fig. 7. Circular dichroism (CD) spectra recorded at 22 °C of complex **4** and/or CT DNA. Individual samples contained 10 mM sodium phosphate buffer pH 7.0 and: 150 μM bp CT DNA (red line); 15 μM complex **4** (black line), or 16 to 91 μM of complex **4** in the presence of 150 μM bp CT DNA (orange, green, blue, and purple lines). Abbreviation: **r** = complex **4** to DNA bp molar ratio = [complex]/[DNA bp]. (For interpretation of the references to color in this figure legend, the reader is referred to the web version of this article.)

comparable experimental conditions, polypyridyl-induced increases in DNA T_m range from 0 °C to 2 °C for the latter binding modes [88,89].

Melting temperature curves for 19 μM bp CT DNA were acquired in the absence and presence of 1 to 24 μM of the trinuclear Cu(II) complex **4** (Fig. 8A). A comparison was then made to the melting curves generated by 3 mol equiv of $CuCl_2$ (Fig. 8B). Rather than engaging in intercalation, copper(II) ions released by copper salts interact with negatively charged oxygen of the phosphate backbone and with nitrogen and oxygen donor atoms in guanine and cytosine bases [60]. At a complex to DNA bp molar ratio approaching the **r** value associated with complete DNA photocleavage (**r** = 0.05 in Fig. 8A vs. **r** = 0.053 in Fig. 2), the addition of **4** to CT DNA increased DNA T_m from 68 °C to 69 °C. An equivalent increase in DNA melting temperature was produced when the complex was replaced with 3 mol equiv. of $CuCl_2$ (**r** = 0.16 in Fig. 8B). While the initial one degree C changes are not statistically significant, the melting temperatures of complex **4** and copper(II) chloride both continued to increase at higher **r** values, reaching maxima of 71 °C and 70 °C, respectively (**r** = 1.26 in Fig. 8A vs. **r** = 3.79 in Fig. 8B). The sharp CT DNA melting transitions and modest melting temperature enhancements exhibited by complex **4** and $CuCl_2$ are consistent with non-intercalative DNA interactions [1,3,88,89].

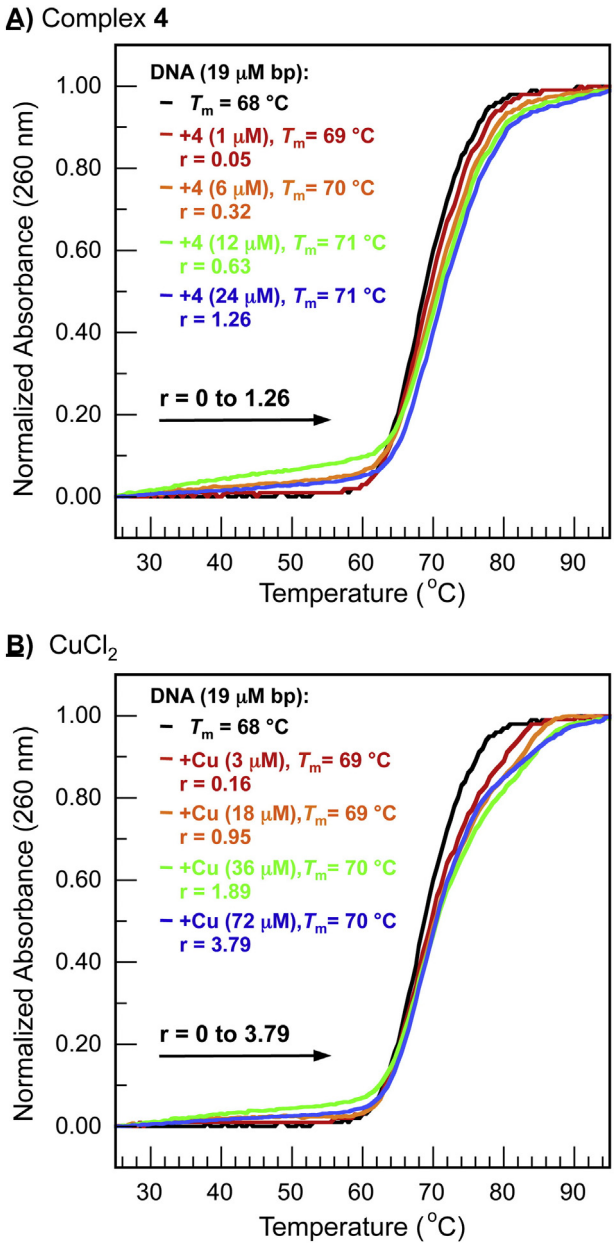

Fig. 8. Normalized thermal melting curves of 19 μM bp CT DNA in the absence and presence of (A) 1 to 24 μM of **4** and (B) 3 to 72 μM of $CuCl_2$ (10 mM sodium phosphate buffer pH 7.0). Abbreviations: **r** = complex **4** (or $CuCl_2$) to DNA bp molar ratio = [compound]/[DNA bp]; T_m = DNA melting temperature.

3.5.4. Fluorescence measurements

Our next attempt to evaluate the association of complex **4** with DNA involved the use of fluorescence spectroscopy. However, a fluorescence spectrum for complex $(Cu(en))_3hat\text{-}(COO)_6$ (**4**) could not be acquired. No emission was observed upon irradiation of the complex, even when CT DNA was present (data not shown). We then examined the effects of **4** on the emission of DNA-bound ethidium bromide (EtBr). Towards this end, EtBr fluorescence quenching assays were conducted for complex **4** along with other potential quenching agents (Q): either ethylenediaminetetraacetate (a negative control that does not bind to DNA), $CuCl_2$, or the classical DNA minor groove binder pentamidine. When intercalated between hydrophobic DNA base pairs, EtBr is highly fluorogenic. However, when displaced from the DNA helix into an aqueous environment, strong quenching occurs due to the transfer of protons from the amino groups of excited singlet state of EtBr to solvent water molecules [90,91]. In typical EtBr experiments, commonly encountered quenching routes include the direct displacement of EtBr from the DNA helix, in addition to two non-displacement based pathways involving either electron transfer [90,92,93] or Förster energy transfer from the excited state of the DNA-bound EtBr to the ground state quencher [92–94].

In the quenching experiments, the fluorescence of 12 μM of EtBr in the presence and absence of 19 μM bp CT DNA was monitored as a function of increasing quencher concentration (**r** = 0.007 to 2.37; Fig. 9). While EtBr emission did not significantly change when DNA was omitted from reactions, in the presence of DNA the fluorescence was quenched in the following order: complex **4** ≫ pentamidine ≫ $CuCl_2$ > EDTA (Fig. 9). The same trend was observed when higher concentrations of quencher were employed (Fig. S12 in Supplementary data). The data in Fig. 9 show that complex **4** was effective in reducing EtBr emission at **r** values associated with complex-sensitized DNA photocleavage (**r** = 0.026 to 0.526 in Fig. 9 vs. **r** = 0.003 to 0.053 in Fig. 2 and **r** = 0.130 to 0.530 in Fig. S7). UV–visible absorption

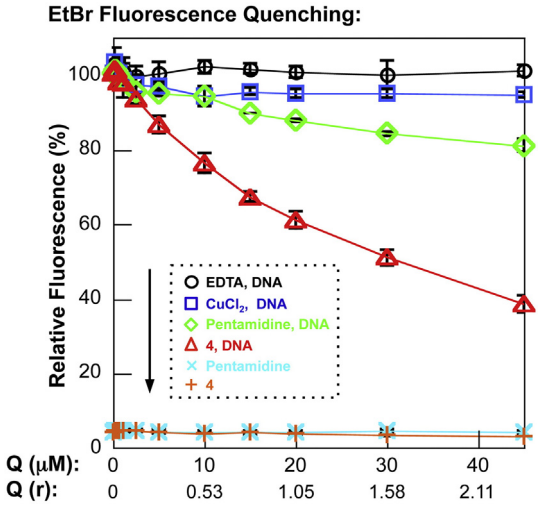

Fig. 9. EtBr fluorescence emission as a function of quencher concentration. In the wells of a microplate, aqueous solutions containing a final concentration of 12 μM of EtBr were equilibrated in the presence and absence of 19 μM bp CT DNA (10 mM of sodium phosphate buffer pH 7.0). A potential quencher (either EDTA, $CuCl_2$, pentamidine or complex **4**) was added at final concentrations ranging from 0.125 μM to 45 μM. The samples were excited at 540 nm and then read for fluorescence at 590 nm. Data are averaged over three trials and error bars show standard deviation. Abbreviations: Q = potential quencher; **r** = Q to DNA bp molar ratio = [Q]/[DNA bp].

spectra recorded for each of the potential quenchers ruled against the possibility that the fluorescence quenching illustrated in Figs. 9 and S12 was the result of absorption of incident irradiation: there was little if any overlap between quencher absorption in the absence and presence of DNA and the 540 nm excitation wavelength used to irradiate the EtBr DNA complex (Fig. S13).

In order to gain a better understanding of the DNA-ligand interactions underlying quenching, the complex **4** data from Fig. 9 were fit to the linear and quadratic forms of the Stern-Volmer equation (Fig. 10). Cases of pure dynamic or pure static fluorescence quenching are best described by the linear Stern-Volmer model ($I_o/I = 1 + K_{SV}[Q]$ [37]), in which plots of I_o/I are linearly dependent on quencher concentration [Q] and I_o and I are equal to fluorescence in the absence and presence of quencher, respectively. When both dynamic and static mechanisms occur simultaneously, plots of I_o/I vs. Q deviate from linearity and are more accurately predicted by a quadratic Stern-Volmer model obtained by multiplying dynamic and static components of the linear equation together ($I_o/I = (1 + K_D[Q])(1 + K_S[Q])$; [38,39]). As shown in Fig. 10, the quadratic form of the Stern-Volmer equation provides a better fit for the complex **4** quenching data in Fig. 9 ($R = 0.9994$; $\chi^2 = 0.0085$ in Fig. 10B).

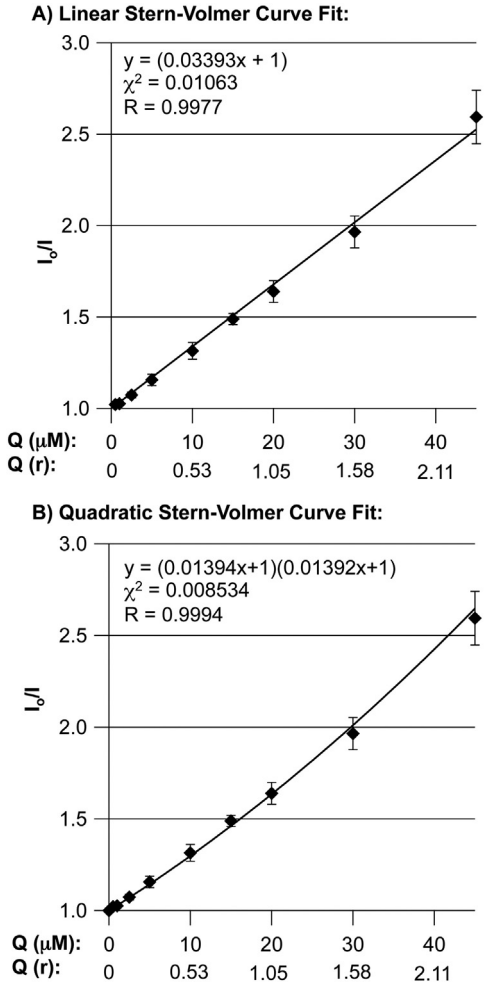

Fig. 10. Stern-Volmer analyses. I_o/I plotted as a function of increasing complex **4** concentration shows quenching of 12 μM of EtBr in the presence of 19 μM bp CT DNA (10 mM sodium phosphate pH 7.0). Individual data points (black diamonds) are from Fig. 9. The black lines are the best fits of the data points to the linear (A) and quadratic (B) Stern-Volmer equations, respectively. Data are averaged over three trials and error bars show standard deviation. Abbreviations: I_o = EtBr fluorescence intensity without quencher; I = EtBr fluorescence intensity with quencher; Q = complex **4**; **r** = Q to DNA bp molar ratio = [Q]/[DNA bp]; R = correlation coefficient; χ^2 = chi-squared test.

The likelihood that complex **4** was quenching fluorescence by directly displacing EtBr from DNA was examined by comparing UV–visible spectra of 12 μM of free EtBr vs. DNA bound EtBr in the presence and absence of increasing concentrations of complex **4** (Fig. S13). In addition to dramatically enhanced fluorescence, EtBr exhibits hypochromicity, and a pronounced red shift in visible absorption upon binding DNA [93]. However, spectral evidence substantiating the release of free EtBr could not be detected at any of the complex **4** concentrations tested (Fig. S13). Quenching by Förster energy transfer could be ruled out because there is minimal if any overlap between complex **4** absorption (Figs. 6, S11, S12) and the emission wavelengths of DNA-bound EtBr (~550 nm to 700 nm) [90]. While the precise mechanism of EtBr fluorescence quenching by complex **4** remains to be elucidated, there are reports in the literature of cobalt(III) polypyridyl and copper(II) macrocyclic complexes that quench the fluorescence of DNA-bound EtBr by direct electron transfer from excited state of the EtBr to the metal ion center of the complex [90]. Notwithstanding, the quadratic Stern-Volmer behavior exhibited by **4** (Fig. 10B) when taken together with the DNA photocleavage (Figs. 2, 3, and S7) and thermal melting data (Fig. 8) presented in this paper, point to a direct interaction between complex **4** and DNA.

4. Conclusions

Herein we have reported the synthesis of the sodium salts of a polydentate hexaazatriphenylene-hexacarboxylate ligand (hat-$(COO^-)_6$; **3**) and its trinuclear Cu(II) complex ($((Cu(en))_3$hat-$(COO)_6$; **4**) (Scheme 1). Irradiation of low, micromolar concentrations of these compounds in the presence of pUC19 plasmid sensitizes DNA photocleavage in near quantitative yields (350 nm, pH 7.0; Figs. 1 to 3, S3). In the case of hat-$(COO^-)_6$ (**3**), photo-oxidative DNA damage was markedly enhanced upon copper(II) addition (Fig. 1A). We had initially considered the trinuclear Cu(II) complex **4** and the parent ligand **3** to be highly unlikely DNA cleaving agents. Upon water solvation of their synthesized sodium salts, **3** and **4** would have a respective tendency to be negatively and neutrally charged at pH 7.0, resulting in low affinity for negatively charged duplex DNA. Moreover, an examination of the structures of **3** and **4** suggests that intercalation of the hexaazatriphenylene ring of each compound into DNA might be sterically hindered by the ligands' pendant carboxylate groups, and in the case of **4**, by the ethylenediamine unit bound to each Cu(II) center of the hat ring. In addition to intercalation, the six carboxylate groups and Cu(II)-bound ethylenediamine units of **4** might have the capacity to prevent DNA minor groove binding, which is normally favored by sterically unhindered aromatic ring systems that can make close van der Waals contacts with the groove walls.

By using chemical additives to probe for reactive oxygen species, we have shown that irradiation of **4** sensitizes high levels of oxidative DNA photocleavage through a process that is likely to involve hydroxyl radicals (Table 1; Figs. S8 and S10). The diffusion radius of hydroxyl radicals is approximately 20 Å [84], suggesting that complex **4** is in close proximity to the DNA helix during photocleavage reactions. The absorption spectrum of the complex and CD spectrum of DNA are unchanged upon the addition of DNA and **4**, respectively (Figs. 6, 7, and S11), indicating that the interaction between complex **4** and DNA is likely to be external in nature. Moreover, there were no ICD signals suggestive of intercalation and/or surface-minor groove binding interactions (Fig. 7). In thermal melting experiments, complex **4** gave rise to a small increase in DNA melting temperature consistent with non-intercalative binding (Fig. 8). Additional evidence for a direct interaction between DNA and **4** was provided by fluorescence experiments in which the complex was shown to efficiently quench the emission of DNA-bound ethidium bromide (Figs. 9 and 10).

When taken together, our experimental data suggest that trinuclear Cu(II) complex **4** associates with DNA in an external fashion. When bound externally, chromophores have more access to oxygen compared

to intercalative and groove binding modes. As a result, DNA damaging reactive oxygen species are generated more efficiently [36,95]. This may be an essential factor that contributes to the ability of **4** to photocleave plasmid DNA in 98% to 99% yield at low micromolar concentrations of complex (**r** = 0.053 and/or 0.026 in Figs. 2, 3, and S3; 350 nm, pH 7.0). At this time, we believe that the mechanism of cleavage may involve the photo-reduction of Cu(II) to Cu(I), with DNA acting as a possible electron donor. Copper(I) may react with ground state triplet oxygen to generate superoxide anion radicals and then DNA-cleaving hydroxyl radicals via a Fenton-type process (Fig. 5). Upon water solvation of the synthesized sodium nitrate salt $[(Cu(en))_3hat\text{-}(COONa)_6](NO_3)_6$ (Scheme 1), free $(Cu(en))_3hat\text{-}(COO)_6$ (**4**) would be expected to be near-neutral in charge at pH 7.0. However, the weak but persistent association of the carboxylate groups of the complex with Na(I) ions from bulk solution and/or from the ion atmosphere surrounding DNA could conceivably induce a templating effect in which **4** acquires positive charge and associates with DNA by external, electrostatic interactions [49–53,55–57].

The utilization of copper-based photo-nucleases is of considerable interest because of copper bioavailability at the cellular level and the high levels of copper found in cancer cells [18–29]. With this being said, our future work will be focused on developing external binding copper photo-nucleases, expressly those that can be activated using long wavelengths of light that are efficiently transmitted through biological tissues (700 nm to 900 nm) [33].

Abbreviations

BCS	bathocuproinedisulfonic acid
bpy	2,2′-bipyridine
CT	calf thymus
dpq	dipyridoquinoxaline
hat	1,4,5,8,9,12-hexaazatriphenylene
EtBr	ethidium bromide
hat-$(COO^-)_6$	1,4,5,8,9,12-hexaazatriphenylene-hexacarboxylate
HEPES	2-[4-(2-hydroxyethyl)piperazin-1-yl]ethanesulfonate
ICD	induced circular dichroism
l	linear DNA
LED	light emitting diode
n	nicked DNA
phen	1,10-phenanthroline
ROS	reactive oxygen species
r	compound to DNA bp molar ratio = [compound]/[DNA bp]
Q	quencher
s	supercoiled DNA
SOD	superoxide dismutase
TAE	tris-acetate EDTA
T_m	DNA melting temperature

Acknowledgments

This work was supported by the Georgia State University Molecular Basis of Disease Program (D.E.W.), the CTQ2011-26822 (A.L.), and the National Science Foundation (CHE-0718634, K.B.G).

Appendix A. Supplementary data

Supplementary data to this article can be found online at http://dx.doi.org/10.1016/j.jinorgbio.2016.12.007.

References

[1] J.M. Kelly, A.B. Tossi, D.J. McConnell, C. OhUigin, Nucleic Acids Res. 13 (1985) 6017–6034.
[2] M.B. Fleisher, K.C. Waterman, N.J. Turro, J.K. Barton, Inorg. Chem. 25 (1986) 3549–3551.
[3] A.B. Tossi, J.M. Kelly, Photochem. Photobiol. 49 (1989) 545–556.
[4] J.-P. Lecomte, A. Kirsch-De Mesmaeker, M.M. Feeney, J.M. Kelly, Inorg. Chem. 34 (1995) 6481–6491.
[5] A. Kirsch-De Mesmaeker, G. Orellana, J.K. Barton, N.J. Turro, Photochem. Photobiol. 52 (1990) 461–472.
[6] C. Moucheron, A. Kirsch-De Mesmaeker, S. Choua, Inorg. Chem. 36 (1997) 584–592.
[7] T.J. Rutherford, O. Van Gijte, A. Kirsch-De Mesmaeker, F.R. Keene, Inorg. Chem. 36 (1997) 4465–4474.
[8] B. Armitage, Chem. Rev. 98 (1998) 1171–1200.
[9] R. Blasius, C. Moucheron, A. Kirsch-De Mesmaeker, Eur. J. Inorg. Chem. (2004) 3971–3979.
[10] K. Szacilowski, W. Macyk, A. Drzewiecka-Matuszek, M. Brindell, G. Stochel, Chem. Rev. 105 (2005) 2647–2694.
[11] B. Elias, A. Kirsch-De Mesmaeker, Coord. Chem. Rev. 250 (2006) 1627–1641.
[12] Y.J. Sun, L.E. Joyce, N.M. Dickson, C. Turro, Chem. Commun. 46 (2010) 2426–2428.
[13] Q.X. Zhou, W.H. Lei, Y. Sun, J.R. Chen, C. Li, Y.J. Hou, X.S. Wang, B.W. Zhang, Inorg. Chem. 49 (2010) 4729–4731.
[14] C. Mari, V. Pierroz, R. Rubbiani, M. Patra, J. Hess, B. Spingler, L. Oehninger, J. Schur, I. Ott, L. Salassa, S. Ferrari, G. Gasser, Chem. Eur. J. 20 (2014) 14421–14436.
[15] H.M. Yin, M. Stephenson, J. Gibson, E. Sampson, G. Shi, T. Sainuddin, S. Monro, S.A. McFarland, Inorg. Chem. 53 (2014) 4548–4559.
[16] S. Swavey, M. DeBeer, K.Y. Li, Inorg. Chem. 54 (2015) 3139–3147.
[17] G. Yang, J.Z. Wu, L. Wang, L.N. Ji, X. Tian, J. Inorg. Biochem. 66 (1997) 141–144.
[18] K. Schumann, H.G. Classen, H.H. Dieter, J. Konig, G. Multhaup, M. Rukgauer, K.H. Summer, J. Bernhardt, H.K. Biesalski, Eur. J. Clin. Nutr. 56 (2002) 469–483.
[19] W.E.C. Wacker, B.L. Vallee, J. Biol. Chem. 234 (1959) 3257–3262.
[20] K.P. Cantor, J.E. Hearst, Proc. Natl. Acad. Sci. U. S. A. 55 (1966) 642–649.
[21] S.E. Bryan, D.L. Vizard, D.A. Beary, R.A. LaBiche, K.J. Hardy, Nucleic Acids Res. 9 (1981) 5811–5823.
[22] P. Fuerst, D. Hamer, Proc. Natl. Acad. Sci. U. S. A. 86 (1989) 5267–5271.
[23] D.J. Thiele, Nucleic Acids Res. 20 (1992) 1183–1191.
[24] V.L. Goodman, G.J. Brewer, S.D. Merajver, Endocr. Cancer 11 (2004) 255–263.
[25] A. Nasulewicz, A. Mazur, A. Opolski, J. Trace Elem. Med. Biol. 18 (2004) 1–8.
[26] L. Finney, S. Vogt, T. Fukai, D. Glesne, Clin. Exp. Pharmacol. Physiol. 36 (2009) 88–94.
[27] A. Gupte, R.J. Mumper, Cancer Treat. Rev. 35 (2009) 32–46.
[28] S.M. Hadi, M.F. Ullah, A.S. Azmi, A. Ahmad, U. Shamim, H. Zubair, H.Y. Khan, Pharm. Res. 27 (2010) 979–988.
[29] R. Safi, E.R. Nelson, S.K. Chitneni, K.J. Franz, D.J. George, M.R. Zalutsky, D.P. McDonnell, Cancer Res. 74 (2014) 5819–5831.
[30] S. Dhar, D. Senapati, P.K. Das, P. Chattopadhyay, M. Nethaji, A.R. Chakravarty, J. Am. Chem. Soc. 125 (2003) 12118–12124.
[31] S. Dhar, D. Senapati, P.A.N. Reddy, P.K. Das, A.R. Chakravarty, Chem. Commun. (2003) 2452–2453.
[32] S. Dhar, M. Nethaji, A.R. Chakravarty, Inorg. Chem. 45 (2006) 11043–11050.
[33] Z.Y. Li, K.B. Grant, RSC Adv. 6 (2016) 24617–24634.
[34] J. Sambrook, F.E. Fritsch, T. Maniatis, Molecular Cloning, A Laboratory Manual, Cold Spring Harbor Press, New York, 1989.
[35] K. Kanakarajan, A.W. Czarnik, J. Organomet. Chem. 51 (1986) 5241–5243.
[36] C.A. Terry, M.-J. Fernandez, L. Gude, A. Lorente, K.B. Grant, Biochemistry 50 (2011) 10375–10389.
[37] J.R. Lakowicz, G. Weber, Biochemistry 12 (1973) 4161–4170.
[38] H.-J. Timpe, G. Isreal, H. Becker, I.R. Gould, N.J. Turro, Chem. Phys. Lett. 99 (1983) 275–280.
[39] A.R. Soemo, J.E. Pemberton, J. Fluoresc. 24 (2014) 295–299.
[40] H. Grove, J. Sletten, M. Julve, F. Lloret, J. Chem. Soc. Dalton Trans. (2001) 1029–1034.
[41] H. Grove, J. Sletten, M. Julve, F. Lloret, L. Lezama, J. Carranza, S. Parsons, P. Rillema, J. Mol. Struct. 606 (2002) 253–265.
[42] S. Kitagawa, S. Masaoka, Coord. Chem. Rev. 246 (2003) 73–88.
[43] A. Rahman, Shahabuddin, S.M. Hadi, J.H. Parish, K. Ainley, Carcinogenesis 10 (1989) 1833–1839.
[44] L. Flowers, S.T. Ohnishi, T.M. Penning, Biochemistry 36 (1997) 8640–8648.
[45] S.U. Rehman, H. Zubair, T. Sarwar, M.A. Husain, H.M. Ishqi, S. Nehar, M. Tabish, Tumour Biol. 36 (2015) 1237–1244.
[46] J.B. Sun, N. Jiang, M.Y. Lv, P. Wang, F.G. Xu, J.Y. Liang, W. Qu, RSC Adv. 5 (2015) 24750–24757.
[47] J.L. Sagripanti, P.L. Goering, A. Lamanna, Toxicol. Appl. Pharmacol. 110 (1991) 477–485.
[48] M.K.M. Rabia, H.A. Al-Gwidi, K.A.A. Al-Ibrahem, Bull. Electrochem. 20 (2004) 139–144.
[49] S. Berto, E. Chiavazza, P. Canepa, E. Prenesti, P.G. Daniele, Phys. Chem. Chem. Phys. 18 (2016) 13118–13125.
[50] L. Vrbka, J. Vondrasek, B. Jagoda-Cwiklik, R. Vacha, P. Jungwirth, Proc. Natl. Acad. Sci. U. S. A. 103 (2006) 15440–15444.
[51] B. Jagoda-Cwiklik, R. Vacha, M. Lund, M. Srebro, P. Jungwirth, J. Phys. Chem. B 111 (2007) 14077–14079.
[52] B. Hess, N.F.A. van der Vegt, Proc. Natl. Acad. Sci. U. S. A. 106 (2009) 13296–13300.
[53] B. Jayaram, F.M. DiCapua, D.L. Beveridge, J. Am. Chem. Soc. 113 (1991) 5211–5215.
[54] N. Korolev, A.P. Lyubartsev, A. Laaksonen, L. Nordenskiold, Biophys. J. 82 (2002) 2860–2875.
[55] Y. Bai, M. Greenfeld, K.J. Travers, V.B. Chu, J. Lipfert, S. Doniach, D. Herschlag, J. Am. Chem. Soc. 129 (2007) 14981–14988.
[56] G.M. Giambasu, M.K. Gebala, M.T. Panteva, T. Luchko, D.A. Case, D.M. York, Nucleic Acids Res. 43 (2015) 8405–8415.
[57] S.P. Meisburger, S.A. Pabit, L. Pollack, Biophys. J. 108 (2015) 2886–2895.

[58] J. Bjerrum, G. Schwarzenbach, L.G. Sillén, Stability Constants of Metal-Ion Complexes, with Solubility Products of Inorganic Substances. Part 1. Organic Ligands, The Chemical Society, London, 1957.
[59] D.V. Djarmati, M.K. Stankovic, Arh. Hig. Rada Toksikol. 38 (1987) 33–36.
[60] C. Zimmer, G. Luck, H. Fritzsche, H. Triebel, Biopolymers 10 (1971) 441–463.
[61] E.A. Sausville, J. Peisach, S.B. Horwitz, Biochemistry 17 (1978) 2740–2746.
[62] E. Rongoni, A. Scafati, M. Matzeu, M. Belli, G. Onori, A. Reale, A. Balerna, A. Bianconi, E. Bernieri, Biopolymers 25 (1986) 217–221.
[63] F. Hutchinson, Mutat. Res. 281 (1992) 261–266.
[64] C.A. Wijker, M.V. Lafleur, Mutat. Res. 429 (1999) 27–35.
[65] M.-J. Fernandez, B. Wilson, M. Palacios, M.-M. Rodrigo, K.B. Grant, A. Lorente, Bioconjug. Chem. 18 (2007) 121–129.
[66] K. Yamamoto, S. Kawanishi, J. Biol. Chem. 264 (1989) 15435–15440.
[67] S. Oikawa, S. Kawanishi, BBA-Gene Struct. Expr. 1399 (1998) 19–30.
[68] B.K. Sinha, F. Leinisch, S. Bhattacharjee, R.P. Mason, Chem. Res. Toxicol. 27 (2014) 674–682.
[69] E.R. Blazek, J.G. Peak, M.J. Peak, Photochem. Photobiol. 49 (1989) 607–613.
[70] T.P. Devasagayam, S. Steenken, M.S. Obendorf, W.A. Schulz, H. Sies, Biochemistry 30 (1991) 6283–6289.
[71] P.K. Sasmal, A.K. Patra, M. Nethaji, A.R. Chakravarty, Inorg. Chem. 46 (2007) 11112–11121.
[72] L.F. Agnez-Lima, J.T. Melo, A.E. Silva, A.H. Oliveira, A.R. Timoteo, K.M. Lima-Bessa, G.R. Martinez, M.H. Medeiros, P. Di Mascio, R.S. Galhardo, C.F. Menck, Mutat. Res. 751 (2012) 15–28.
[73] B. Schwartz, A.K. Olgin, J.P. Klinman, Biochemistry 40 (2001) 2954–2963.
[74] G.A. Juda, E.M. Shepard, B.O. Elmore, D.M. Dooley, Biochemistry 45 (2006) 8788–8800.
[75] J. Cadet, T. Delatour, T. Douki, D. Gasparutto, E.-P. Pouget, J.-L. Ravanat, S. Sauvaigo, Mutat. Res. 424 (1999) 9–21.
[76] N. Paillous, P. Vicendo, J. Photochem. Photobiol. B 20 (1993) 203–209.
[77] Y. Nakabayashi, Y. Watanabe, T. Nakao, O. Yamauchi, Inorg. Chim. Acta 357 (2004) 2553–2560.
[78] C. Cantor, P.R. Schimmel, Biophysical Chemistry, W.H. Freeman, San Francisco, CA, 1980.
[79] R. Ruiz, B. García, J. García-Tojal, N. Busto, S. Ibeas, J.M. Leal, C. Martins, J. Gaspar, J. Borrás, R. Gil-García, M. González-Alvarez, J. Biol. Inorg. Chem. 15 (2010) 515–532.
[80] S.M.M. de Almeida, E.A. Lafayette, L.P.B.G. da Silva, C.A.D. Amorim, T.B. de Oliveira, A.L.T.G. Ruiz, J.E. de Carvalho, R.O. de Moura, E.I.C. Beltrao, M.D.A. de Lima, L.B. de Carvalho, Int. J. Mol. Sci. 16 (2015) 13023–13042.
[81] S.U. Rehman, Z. Yaseen, M.A. Husain, T. Sarwar, H.M. Ishqi, M. Tabish, PLoS One 9 (2014) 93913.
[82] T. Sarwar, M.A. Husain, S.U. Rehman, H.M. Ishqi, M. Tabish, Mol. BioSyst. 11 (2015) 522–531.
[83] J. Ramesh, S. Sujatha, C. Arunkumar, RSC Adv. 6 (2016) 63271–63285.
[84] T. Hoshi, S. Heinemann, J. Physiol. 531 (2001) 1–11.
[85] N.C. Garbett, P.A. Ragazzon, J.B. Chaires, Nat. Protoc. 2 (2007) 3166–3172.
[86] B.B. Johnson, K.S. Dahl, I. Tinoco Jr., V.I. Ivanov, V.B. Zhurkin, Biochemistry 20 (1981) 73–78.
[87] A. Silvestri, G. Barone, G. Ruisi, M.T. Lo Giudice, S. Tumminello, J. Inorg. Biochem. 98 (2004) 589–594.
[88] N. Chitrapriya, Y.J. Jang, S.K. Kim, H. Lee, J. Inorg. Biochem. 105 (2011) 1569–1575.
[89] B. Maity, S. Gadadhar, T.K. Goswami, A.A. Karande, A.R. Chakravarty, Dalton Trans. 40 (2011) 11904–11913.
[90] C.L. Liu, J.Y. Zhou, H.B. Xu, J. Inorg. Biochem. 71 (1998) 1–6.
[91] A.J. Geall, I.S. Blagbrough, J. Pharm. Biomed. Anal. 22 (2000) 849–859.
[92] S.J. Atherton, P.C. Beaumont, J. Phys. Chem. 90 (1986) 2252–2259.
[93] R.F. Pasternack, M. Caccam, B. Keogh, T.A. Stephenson, A.P. Williams, E.J. Gibbs, J. Am. Chem. Soc. 113 (1991) 6835–6840.
[94] B.C. Baguley, M. Le Bret, Biochemistry 23 (1984) 937–943.
[95] B. Åkerman, E. Tuite, Nucleic Acids Res. 24 (1996) 1080–1090.